ARTICLE
Journal of Cellular Biochemistry 111:295–309 (2010)

Journal of Cellular Biochemistry

Temporal and Spatial Expression of Osteoactivin During Fracture Repair

Samir M. Abdelmagid,[1] Mary F. Barbe,[1,2] Michael Hadjiargyrou,[3] Thomas A. Owen,[4] Roshanak Razmpour,[1] Saqib Rehman,[5] Steven N. Popoff,[1,5] and Fayez F. Safadi[1,5,6*]

[1]*Department of Anatomy and Cell Biology, Temple University School of Medicine, Philadelphia, Pennsylvania*
[2]*Department of Physical Therapy, Temple University, Philadelphia, Pennsylvania*
[3]*Department of Biomedical Engineering, Stony Brook University, Stony Brook, New York*
[4]*Theoretical and Applied Science, Ramapo College of New Jersey, Mahwah, New Jersey*
[5]*Department of Orthopaedic Surgery and Sports Medicine, Temple University Hospitals, Philadelphia, Pennsylvania*
[6]*Department of Otolaryngology—Head and Neck Surgery, Temple University Hospitals, Philadelphia, Pennsylvania*

ABSTRACT

We previously identified osteoactivin (OA) as a novel secreted osteogenic factor with high expression in developing long bones and calvaria, and that stimulates osteoblast differentiation and matrix mineralization in vitro. In this study, we report on OA mRNA and protein expression in intact long bone and growth plate, and in fracture calluses collected at several time points up to 21 days post-fracture (PF). OA mRNA and protein were highly expressed in osteoblasts localized in the metaphysis of intact tibia, and in hypertrophic chondrocytes localized in growth plate, findings assessed by in situ hybridization and immunohistochemistry, respectively. Using a rat fracture model, Northern blot analysis showed that expression of OA mRNA was significantly higher in day-3 and day-10 PF calluses than in intact rat femurs. Using in situ hybridization, we examined OA mRNA expression during fracture healing and found that OA was temporally regulated, with positive signals seen as early as day-3 PF, reaching a maximal intensity at day-10 PF, and finally declining at day-21 PF. At day-5 PF, which correlates with chondrogenesis, OA mRNA levels were significantly higher in the soft callus than in intact femurs. Similarly, we detected high OA protein immunoexpression throughout the reparative phase of the hard callus compared to intact femurs. Interestingly, the secreted OA protein was also detected within the newly made cartilage matrix and osteoid tissue. Taken together, these results suggest the possibility that OA plays an important role in bone formation and serves as a positive regulator of fracture healing. J. Cell. Biochem. 111: 295–309, 2010.

KEY WORDS: FRACTURE; OSTEOACTIVIN; OSTEOBLASTS; CHONDROCYTES; GROWTH PLATE

Bone tissue is highly mineralized, undergoes continuous remodeling, and retains the potential to regenerate throughout adult life [Reddi, 1998a,b; Olsen et al., 2000]. Bone tissue has three major cell types: bone-forming osteoblasts, bone-resorbing osteoclasts, and osteocytes. Osteoblasts are derived from the mesenchymal stem cells (MSCs), which can also differentiate into myocytes, adipocytes, and chondrocytes in differentiation permissive conditions, whereas osteoclasts are derived from stem cells coming from the monocytic lineage [Wang et al., 1993; Yamaguchi, 1995].

The reparative process of bone fracture involves a series of events that include migration, proliferation, differentiation, and activation of several cell types including mesenchymal and hematopoietic stem cells that ultimately lead to bone formation and remodeling toward the original shape [Einhorn, 1998; Gittens and Uludag, 2001; Mandracchia et al., 2001; Gerstenfeld et al., 2003]. Bone formation at fracture sites can occur via two distinct processes; intramembranous and endochondral. Intramembranous ossification typically occurs in stabilized bone fracture segments, where MSCs directly differentiate into osteoblasts, similar to what occurs during the

The authors have no conflict of interest.
Grant sponsor: National Institute of Arthritis and Musculoskeletal and Skin Diseases; Grant number: AR48892.
*Correspondence to: Prof. Fayez F. Safadi, PhD, Associate Professor, Vice Chairperson for Research, Department of Anatomy and Cell Biology, Temple University School of Medicine, 3400 North Broad Street, Philadelphia, PA 19140. E-mail: fsafadi@temple.edu
Received 27 April 2010; Accepted 29 April 2010 • DOI 10.1002/jcb.22702 • © 2010 Wiley-Liss, Inc.
Published online 19 May 2010 in Wiley Online Library (wileyonlinelibrary.com).

development of the flat bones of the skull. Endochondral ossification typically occurs in biomechanically unstable fracture segments, where bone formation involves an intermediary cartilage model, similar to the development of long bones [Gittens and Uludag, 2001; Mandracchia et al., 2001; Thompson et al., 2002].

Various growth factors are expressed during fracture healing, such as bone morphogenetic proteins (BMPs), transforming growth factor beta (TGF-β), fibroblast growth factors (bFGFs), and platelet-derived growth factors (PDGFs) [Sandberg et al., 1993; Tatsuyama et al., 2000; Schmid et al., 2009]. Their expression suggests a possible role for these factors in bone formation and repair, and in fact, each of these growth factors has been shown to stimulate bone healing in animal fracture models [Andriano et al., 2000; Gittens and Uludag, 2001; Wong et al., 2003; Chen et al., 2004]. New growth factors important during fracture healing are being investigated, and in this study, we report on a novel osteogenic factor, osteoactivin (OA), and its relative temporal and spatial expression during fracture healing.

Using differential gene display, we initially identified OA by virtue of its overexpression in bones from osteopetrotic rats compared to their normal littermates [Safadi et al., 2001; Owen et al., 2003]. RT-PCR analysis showed marked increase in OA expression in intact long bones and calvaria compared to other organs, and in primary osteoblast cultures from wild-type rats [Safadi et al., 2001; Owen et al., 2003]. OA has been reported under different names in other cell types including dendritic cell heparan sulfate proteoglycan integrin-dependent ligand (DC-HIL) in dendritic and T cells [Shikano et al., 2001; Chung et al., 2007], human hematopoietic growth factor inducible neurokinin (HGFIN) in tumor cells [Bandari et al., 2003], and glycoprotein nmb (GPnmb) in melanoma cell lines [Weterman et al., 1995; Okamoto et al., 2005; Kuan et al., 2006; Tse et al., 2006; Pollack et al., 2007] and melanocytes [Anderson et al., 2002, 2006]. OA functions to regulate cell proliferation, adhesion, differentiation, and biosynthesis of extracellular matrix (ECM) proteins in various cell types under both normal and pathological conditions [Safadi et al., 2001; Shikano et al., 2001; Ahn et al., 2002; Anderson et al., 2002, 2006; Mo et al., 2003; Onaga et al., 2003; Owen et al., 2003; Rich et al., 2003; Haralanova-Ilieva et al., 2005; Lennerz et al., 2005; Ogawa et al., 2005; Kuan et al., 2006; Tse et al., 2006; Abdelmagid et al., 2007, 2008; Abe et al., 2007; Chung et al., 2007; Nakamura et al., 2007; Pollack et al., 2007]. For example, OA transgenic mice showed that OA functions as an activator for matrix metalloproteinases (MMP-3 and MMP-9) in fibroblasts infiltrating denervated skeletal muscles [Ogawa et al., 2005]. Another group demonstrated in OA transgenic rats that overexpression of OA in liver cells attenuates the development of hepatic fibrosis [Abe et al., 2007]. Mice with a natural mutation in the OA gene, caused by a premature stop codon that produces a truncated OA protein, develop an eye phenotype with iris pigmentary dispersion and stromal atrophy [Anderson et al., 2001, 2002, 2006]. We have shown that bone marrow mesenchymal cells isolated from OA mutant long bones are defective in their ability to differentiate into osteoblasts compared to their wild-type cells in vitro [Abdelmagid et al., 2008].

We were the first group to report on the expression and function of OA in bone, and have previously shown that OA mRNA and protein exhibit a temporal pattern of expression during differentiation of human and rodent osteoblasts in vitro, with the highest levels during later stages of osteoblast differentiation and matrix mineralization [Safadi et al., 2001; Owen et al., 2003; Abdelmagid et al., 2007]. We have also reported on the role of OA protein in osteoblast differentiation in vitro, where we showed it stimulates production of alkaline phosphatase (ALP) activity, nodule formation, osteocalcin production, and matrix mineralization, without affecting cell proliferation or viability [Selim et al., 2003; Abdelmagid et al., 2007, 2008]. In addition, we demonstrated that OA is downstream of BMP-2, in that it is capable of mediating the effects of BMP-2, at least in part, on osteoblast differentiation and function [Abdelmagid et al., 2007].

Since we have previously identified OA as an anabolic bone factor that stimulates osteoblast differentiation and culture mineralization in vitro [Safadi et al., 2001; Owen et al., 2003; Abdelmagid et al., 2007, 2008], we were interested in elucidating the role of OA in osteopathic stressful conditions as in fracture repair. Therefore, in this study, we examined OA expression in a rat model at several time points post-fracture (PF). We show increased levels of OA mRNA and protein in fracture calluses, using Northern blot and immunohistochemical analyses. We also show that OA mRNA and protein are expressed in different cell types, in intact bone, and in the healing callus PF. The data presented here suggest that OA may work as a positive regulator of bone formation and repair PF in vivo.

MATERIALS AND METHODS

FRACTURE MODEL

All methods and animal procedures were reviewed and approved by Temple University's Lab Animal Users Committee and met guidelines for the use of animals in research. The rat femur fracture model was based on that of Bonnarens and Einhorn [1984]. Briefly, 8-week-old Sprague–Dawley male rats were anesthetized before surgery and their right hind leg was prepared for aseptic surgery. The knee was flexed, and 1 cm incision was made medial to the patellar groove of the femoral condyle. The patella was retracted out of the groove to rest lateral to the condyle. This procedure permitted visualization of the entire articular surface of the distal femur. A hole was drilled through the medullary canal of the femur using a cannula (diameter 0.4 mm). A wider cannula (0.6 mm) was then inserted into this hole. The sharp end of the cannula had been previously blunted to avoid penetration through the hip. The cannula was then cut off, so that the bit remained inside the bone. After this procedure, the distal, cut surface of the cannula lay beneath the femoral groove, allowing the patella to glide unhindered back into place. At this point, the wound was sutured and stapled closed. After completion of the intramedullary nailing, an impact device [Bonnarens and Einhorn, 1984] was used to create a controlled closed-transverse diaphyseal femur fracture. Immediately after fracture production, radiographs were taken to ensure a clean, simple transverse fracture, which was well immobilized by the cannula and remained reduced. A total of 36 animals were prepared in such a manner and euthanized at 3, 5, 7, 10, 14, and 21 days PF ($n = 6$/time point) after death by CO_2 inhalation. From 18 animals, the fracture calluses were collected ($n = 3$/time point PF), dissected free from soft tissues, and processed for RNA extraction. For the

remaining 18 animals (n = 3/time point PF), the fractured femur was removed and processed for in situ hybridization and immunohistochemistry. It is important to note that non-fractured femurs from three control rats were harvested at day 21 to avoid the effect of animal age on changes in OA gene expression.

RNA ISOLATION AND PURIFICATION

As described above, the total RNA was isolated from the intact and fractured femurs (which included the cortical bone or fracture callus, bone marrow, and growth plate cartilage) of Sprague–Dawley male rats using TRizol (Invitrogen, Austin, TX). The intact femurs were initially ground in liquid nitrogen using a mortar and pestle, and then added to the TRizol. In contrast, each callus was added directly to the TRizol. Each sample was homogenized and extracted once with acid–phenol–chloroform using centrifugation (10,000*g*). The aqueous phase was transferred to a fresh tube, mixed with an equal volume of isopropanol, and incubated at −20°C for 24 h to precipitate the RNA. Finally, the RNA was pelleted by centrifugation (10,000*g*), washed with 70% ethanol, air dried, and dissolved in DPEC RNase-free water. The concentration of each RNA sample was determined using a spectrophotometer and the integrity of all RNA samples was monitored on 1% formaldehyde gels.

NORTHERN BLOT ANALYSIS

Total RNA (20 μg) from three samples per time point PF was prepared, fractionated on a 1% formaldehyde/agarose gel, transferred to a nylon membrane (Nytran), and UV cross-linked according to standard procedures. OA cDNA probes were random-labeled with ^{32}P-deoxycytosine triphosphate (dCTP) and hybridized to the membrane at 65°C overnight in a solution containing 15% formamide, 200 mM $NaPO_4$ (pH 7.2), 1 mM EDTA, 7% sodium dodecyl sulfate (SDS), and 1% bovine serum albumin (BSA). After hybridization, the blot was washed in a solution of 2× SSC/1% SDS at 50°C for 30 min, 0.2× SSC/1% SDS at 50°C for 30 min, and 0.2× SSC/0.1% SDS at 65°C for 30 min. Finally, the blot was exposed to Kodak Biomax film at −80°C. The amount of bound probe was quantified by scanning the X-ray film, and the integrated optical density (IOD) of each band measured using Image-J software (NIH, Bethesda, MD). The values of bound OA mRNA were normalized to the corresponding levels of 18S ribosomal RNA (rRNA; on membrane) and plotted as the ratio of OA to 18S rRNA in arbitrary units.

SYNTHESIS OF OA RIBOPROBE

An OA cDNA fragment of 700 bp of the untranslated 3′ end of the rat OA was cloned into a PCR script plasmid vector flanked by the T3 and T7 promoters to generate OA sense and OA antisense riboprobes. The sense and antisense probes were in vitro translated and labeled with digoxygenin (DIG)-modified UTP according to the manufacturer's protocol (Roche Diagnostic Corp., IN). Concentration of the sense and antisense riboprobe was determined using an in situ hybridization labeling kit (Roche Diagnostic Corp.).

IN SITU HYBRIDIZATION OF OA

Tibiae from 2-week-old Sprague–Dawley male rats (n = 3), and from the intact and fractured femurs in Sprague–Dawley male rats (8 weeks old at time of the fracture) at 3, 5, 7, 10, 14, and 21 days PF, were harvested, fixed in 4% paraformaldehyde, decalcified, embedded, and sectioned into 5 μm longitudinal sections and placed on charged slides (Fisher Scientific, Fair Lawn, NJ). Briefly, sections were then baked at 60°C for 1 h, cleared in xylene, and rehydrated with ethanol in PBT (PBS, 0.1% Triton X-100). Sections were treated with Proteinase K (10 mg/ml) in PBT for15 min, and then refixed in 0.2% glutaraldehyde with 4% parafomaldehyde in PBT for 10 min. Sections were placed in a humidified chamber and prehybridized (50% formamide; 5× SSC; 2% blocking powder; 1 mg/ml yeast RNA; 5 mM EDTA; and 50 mg/ml heparin) for 4 h at 60°C. Sections were hybridized (prehybridization solution and either sense or antisense OA-riboprobe at 5 ng/ml) at 60°C overnight. The next day, sections were washed with 100% solution 1 (50% formamide, 5× SSC, 0.1% Triton, and 0.5% CHAPS); 75% solution 1 in 2× SSC; 50% solution 1 in 2× SSC, and 25% solution 1 in 2× SSC. Sections were rewashed with 2× SSC and 0.1% CHAPS twice at 65°C; 0.2× SSC and 0.1% CHAPS twice at 65°C and twice with TBT (0.05 M Tris (pH 7.5), 0.1% Triton, 150 mM NaCl). Sections were blocked with 10% sheep serum, 2% BSA in TBT for 1 h and incubated overnight with anti-DIG antibody (dilution of 1:500 in 10% sheep serum, 2% BSA in TBT). Following antibody treatment, sections were washed as follows: three times with 0.1% BSA in TBT, twice with TBT, three times with Genius buffer (Genius buffer; 100 mM NaCl, 100 mM Tris–HCl, 50 mM $MgCl_2$, pH 9.5, and 0.1% Tween 20). Signals were developed using the color developing solution (45 ml NBT and 35 ml X-phosphate in 10 ml of Genius buffer); sections were covered and placed in the dark until color change has been observed. Color signals were fixed with 4% paraformaldehyde in PBT overnight at 4°C and sections were coverslipped with PBS-80% glycerol as a mounting medium, and examined using a Nikon-Eclipse E800 light microscope.

GENERATION OF OA ANTIBODY

Antibody specific to OA (OA-551) was generated against the peptide sequence of amino acids 551–568. Several OA peptides were screened and the specific peptide sequence was selected based on its potential antigenicity and the lack of homology with other peptide sequences in the protein database bank. Chickens were immunized, and the crude precipitated IgY crude was purified by affinity chromatography on Sepharose 4B derivatized with the immunizing peptide (Cambridge Research Biochemicals, Stockton-Tees, UK).

IMMUNOHISTOCHEMICAL LOCALIZATION OF OA

Sections of the above-described decalcified and paraffin-embedded tibiae from 2-week-old Sprague–Dawley rats, and from the intact and fractured femurs in Sprague–Dawley male rats (8 weeks old at time of the fracture) at 3, 5, 7, 10, 14, and 21 days PF, were dried overnight at room temperature (RT) after placement onto charged slides (described above). Sections were then immersed in xylene for 5 min to dissolve the paraffin, and then rehydrated through graded ethanol to ddH_2O. Sections were incubated with 3% hydrogen peroxide (Fisher Scientific) for 1 h to inhibit endogenous peroxidase activity, rinsed in ddH_2O, and then incubated with 0.4% pepsin (Fisher Scientific) for 20 min. Sections were incubated with donkey serum (4% serum in phosphate buffer), for 1 h, and then primary OA

antichicken antibody (OA-551) was added at a dilution of 1:500 in the blocking serum overnight at RT. The next day, sections were washed in PBS for four times on a shaker, then horseradish peroxidase (HRP)-conjugated donkey antichicken antibody (Jackson Immunoresearch) or fluorescein-tagged donkey antichicken antibody (Jackson Immunoresearch) was applied at a dilution of 1:250, for 2 h at RT. To detect the HRP tag, after washing in PBS, DAB urea solution (Fisher Scientific) was added until a brown reaction product was detected after 5 min. Sections were then rinsed in ddH_2O and counterstained lightly with hematoxylin, dehydrated, coverslipped with DPX mounting media, and examined using a Nikon-Eclipse E800 light microscope. Fluorescent stained sections were washed well with PBS, coverslipped with PBS–80% glycerol as a mounting medium, and examined using a Nikon-Eclipse E800 epifluorescent microscope.

HEMATOXYLIN AND EOSIN, AND MASSON'S TRICHROME STAINING

Sections of the above-described decalcified and paraffin-embedded intact and fractured femurs in Sprague–Dawley male rats (8 weeks old at time of the fracture) at 5, 7, and 10 days PF were immersed in xylene for 5 min to dissolve the paraffin and then rehydrated. Subsets of sections were then stained with hematoxylin and eosin (H&E). Other subsets underwent Masson's trichome staining as follows. Sections were stained in Biebrich scarlet-acid fuchsin solution for 15 min and then rinsed in ddH_2O. Sections were incubated in phosphomolybdic–phosphotungstic acid solution for 15 min and then transferred directly (without rinse) to aniline blue solution and stained for 5–10 min. Sections were then rinsed in ddH_2O and washed in 1% acetic acid solution for 2–5 min and then rinsed in ddH_2O. Stained sections were dehydrated, coverslipped with DPX as a mounting medium, and examined using a Nikon-Eclipse E800 light microscope.

IMAGE ANALYSIS

To quantify the changes in OA mRNA signal and immunoreactive product in the fracture callus, in situ and HRP-DAB stained slides were quantified using a Nikon E800 microscope interfaced with a digital camera (Retiga) and a bioquantification software system (Bioquant Osteo II, Nashville, TN). Prior to acquisition, the camera was white-balanced to ensure that uniform background color was maintained. The microscope's light intensity was maintained at a constant level to ensure the background values were similar for each acquired image. Sections that underwent in situ hybridization for OA mRNA or HRP-DAB immunostaining for OA protein were quantified. Three to five sections per rat intact femur and fracture callus were quantified for each time point PF. Six different microscope fields were measured per section and per rat for OA mRNA or protein expression. Measurements were made only within the boundaries of the sectioned intact and/or fractured cortical bone and surrounding periosteum using the Irregular Region of Interest Option (ROI) of the Bioquant software. The Videocount Area Array option of the Bioquant software was also utilized for these measurements. Videocount area is defined as the number of pixels in a field that meet a user-defined color threshold of staining multiplied by the area of a pixel at the selected magnification. Percent area fractions of hybridized OA mRNA signal or OA immunoreactive product were calculated by dividing the videocount area containing pixels at or above the defined background threshold by the videocount area of the total number of pixels in the chosen field (ROI), and multiplying by 100.

STATISTICAL ANALYSIS

Analysis of variance (ANOVA) was used to evaluate the differences in OA in situ hybridization or immunohistochemical expression at the various time points PF. In the event of a significant group effect, individual pairs of means were compared using Dunnett's post hoc test. A P-value ≤ 0.05 was considered statistically significant. Group means $\pm$ standard error of the mean (SEM) were listed in Table I.

RESULTS

LOCALIZATION OF OA IN INTACT BONE

Previous studies by our laboratory using RT-PCR and Northern blot analyses demonstrated high expression of OA gene in bone and primary osteoblast cultures [Safadi et al., 2001; Owen et al., 2003]. To identify the cellular origin of OA in intact bone, we further extended our analysis to localize OA mRNA and protein in actively growing bone. For this purpose, we used 2-week-old male rat Tibiae since the skeleton is actively growing at this age with increased osteoblast activity. The sense riboprobe (control) showed no signal (Fig. 1A), while the DIG-labeled OA antisense riboprobe clearly showed dark blue signal indicating the expression of OA mRNA in osteoblasts lining the metaphyseal bony trabeculae found directly below the epiphyseal growth plate (Fig. 1B,C). A less intense signal was also detected in newly formed osteocytes trapped within the bone matrix as well as in some cells within the bone marrow (Fig. 1D).

Confirmation of the in situ hybridization data was provided by immunohistochemical localization of OA. We used an anti-OA antibody designed against the C-terminal portion of the protein and

TABLE I. Bioquant Analysis of OA Expression Levels in the Healing Callus at Different Time Points PF

OA level (mean $\pm$ SEM)	No fracture	3 days	5 days	7 days	10 days	14 days	21 days
In situ hybridization	3.76 ± 0.84 (100)	$15.82 \pm 2.09^{*}$ (420)	$14.16 \pm 2.65^{*}$ (376)	$12.71 \pm 2.74^{*}$ (338)	$19.11 \pm 3.64^{*}$ (508)	$7.72 \pm 0.65^{**}$ (205)	$6.09 \pm 0.98^{**}$ (162)
Immunohistochemistry	2.68 ± 0.32 (100)	$8.76 \pm 2.27^{*}$ (327)	$8.08 \pm 0.87^{**}$ (301)	$6.29 \pm 0.54^{**}$ (235)	$11.10 \pm 2.09^{*}$ (414)	$5.85 \pm 0.62^{**}$ (218)	3.54 ± 0.76 (132)

Numbers represent mean $\pm$ SEM of OA signals in nine separate sections of the healing calluses at each time point PF.
$^{*}P < 0.05$, $^{**}P < 0.01$ when expression of OA signals in PF calluses was compared to control (no fracture). Control = 100%.

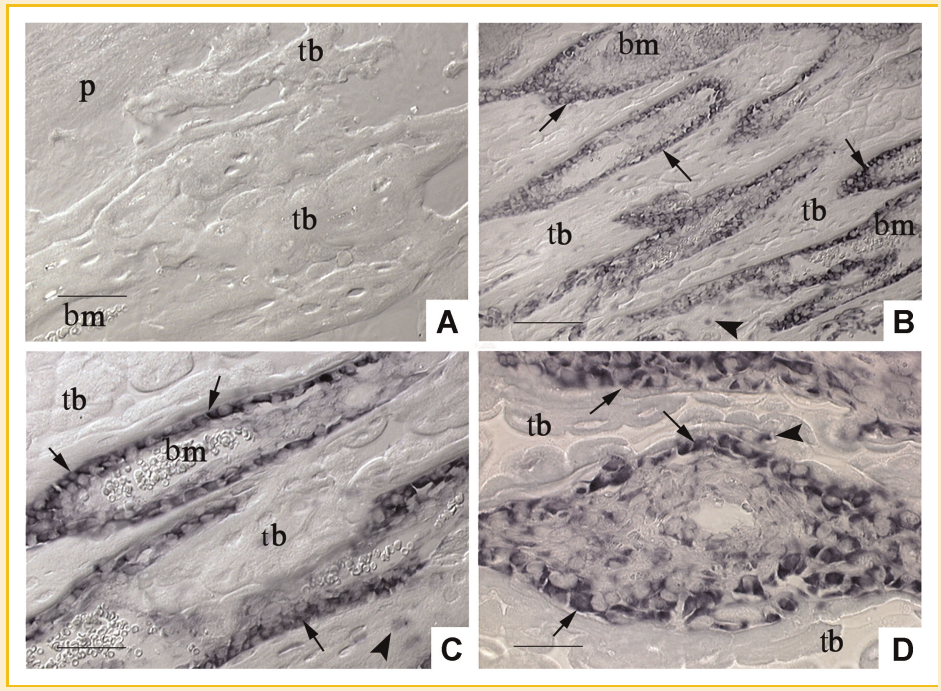

Fig. 1. In situ hybridization (ISH) of OA in long bone. Sections of the proximal tibial metaphyses were processed for ISH with DIG-labeled probe specific for OA. A: Sections incubated with OA sense riboprobe were used as negative control. Note the absence of any positive signal. Image was captured using DIC microscopy. B–D: Photomicrographs of sections hybridized with the OA antisense riboprobe. Note that dark blue positive signals, indicative of OA mRNA expression, were predominantly localized in osteoblasts (arrows) lining the bony trabeculae, whereas fainter signals were seen in osteocytes (arrowheads). tb, trabecular bone; bm, bone marrow; p, periosteum. Scale bar shown (50 μM). [Color figure can be viewed in the online issue, which is available at wileyonlinelibrary.com.]

designated OA-551 Ab. This antibody was shown previously to specifically bind to OA in Western blot and immunofluorescent staining [Owen et al., 2003; Abdelmagid et al., 2007, 2008]. The resulting peroxidase signals clearly showed that this antibody detects OA in active osteoblasts, some osteocytes, and other cells within the bone marrow with the signal specifically located in the cytoplasm (Fig. 2B,C). There was no nuclear signal as evidenced by the absence of OA protein expression in the nucleus. As a control, an adjacent sections were incubated with secondary antibody only and resulted in sections that were completely devoid of labeling (Fig. 2A). Immunofluorescent detection showed similar results (Fig. 2D). Collectively, these data demonstrate that OA mRNA and protein were expressed by osteoblasts lining active bone formation surfaces, with a more limited expression in osteocytes and dispersed cells within the bone marrow spaces, suggesting a potential role for OA in osteoblastogenesis.

LOCALIZATION OF OA IN EPIPHYSEAL GROWTH PLATE

Previous studies reported on the expression of growth factors such as BMPs, TGF-β, bFGF, and PDGF not only in osteoblasts lining the metaphyseal bone trabeculae but also in chondrocytes within the epiphyseal growth plate in vivo [Sandberg et al., 1988; Andrew et al., 1995; Origuchi et al., 1998; Ogawa et al., 2003]. To explore the expression of OA mRNA in chondrocytes, tibiae from 2-week-old male rats were used. Sections at the epiphyseal growth plate cartilage were hybridized with OA antisense riboprobe and clearly demonstrated positive staining for OA mRNA in the zones of early hypertrophic, hypertrophic, and terminally differentiated mineralizing chondrocytes, whereas the zones of proliferating chondrocytes showed no staining (Fig. 3A–C). As a control, sections incubated with OA sense riboprobe (control) showed no signal (Fig. 1D). These data were supported by immunostaining of the OA protein in chondrocytes using OA Ab-551. Immunohistochemical staining of OA protein was detected in the zones containing early and late hypertrophic chondrocytes (Fig. 3F–H). No signal for OA protein was detected in the proliferating zones. In addition, faint signal for OA protein was detected in the cartilaginous matrix surrounding the hypertrophic chondrocytes. As a control, an adjacent section was incubated with secondary antibody only and resulted in no protein labeling (Fig. 3E). In conclusion, these data show that OA mRNA and protein are expressed by hypertrophic chondrocytes in the epiphyseal growth plate cartilage, suggesting a role for OA in chondrogenesis.

HISTOLOGICAL ANALYSIS OF POST-FRACTURE CALLUS

Based on the above data showing increased OA expression in osteoblasts and hypertrophic chondrocytes, we hypothesized that OA is highly expressed wherever active osteogenesis is occurring, such as during fracture repair. Therefore, we used 8-week-old male rats in a fracture-healing model. Femurs were fractured, healing calluses collected at different time points PF, and then stained with

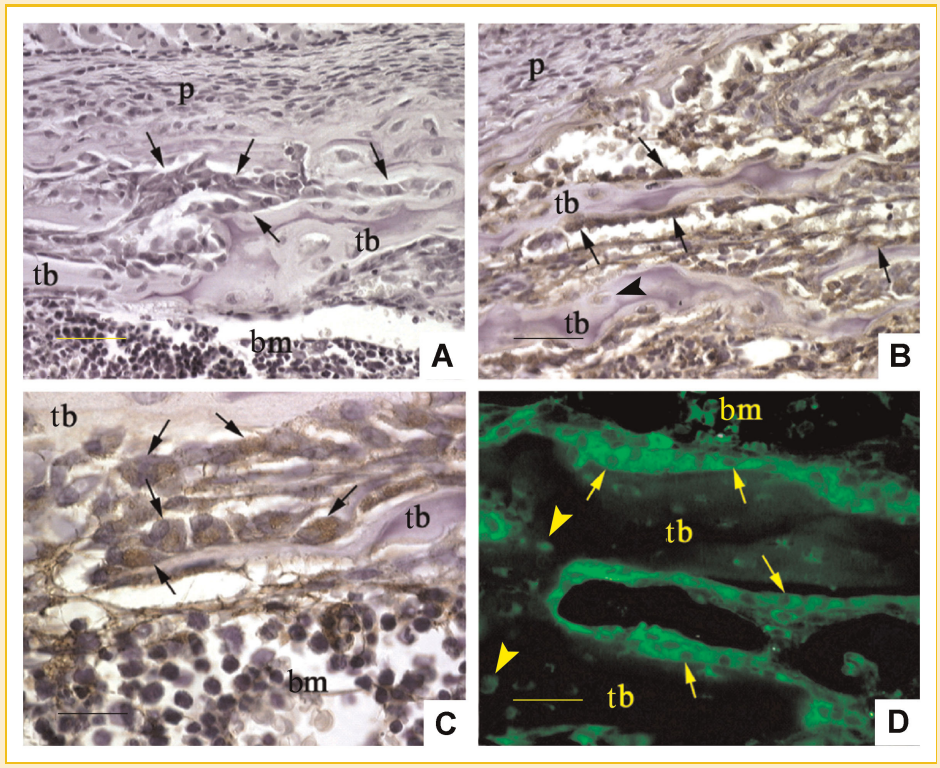

Fig. 2. Immunolocalization of OA in long bone. Sections of the proximal tibial metaphyses were immunostained with antibodies specific for OA. Immunoperoxidase (A–C) and immunofluorescent (D) localization of OA in proximal tibial metaphysis of 2-week-old normal rats. In (A–C) the immunoreaction product had a brown color signal; sections are lightly counterstained with hematoxylin. A: Section representing a negative control where section was not incubated with OA antibody. Note the absence of any reaction product. B,C: Photomicrographs of sections incubated with antibody directed against OA (Ab-551). Note that immunoperoxidase product (B,C) or immunofluorescent staining (D) was predominantly associated with rows of osteoblasts (arrows) lining the bony trabeculae, whereas fainter signals were seen in osteocytes (arrowheads). tb, trabecular bone; bm, bone marrow; p, periosteum. Scale bar shown (50 μM). [Color figure can be viewed in the online issue, which is available at wileyonlinelibrary.com.]

H&E (Fig. 4) and Masson's trichrome (Fig. 5). At the 5-day time point PF, the fractured bone fragments were still separated from each other although the healing callus had begun to form (Fig. 4A,B). We also noticed an increase in aggregated small MSCs, stained with hematoxylin, invading and surrounding the fracture site (Fig. 4C). At the 7-day time point PF, the healing callus was more developed and obliterated the bone marrow cavity (Fig. 4D). The healing callus at 7-day time point PF also demonstrated that focal cartilaginous differentiation (blue staining) had begun, based on cell morphology, with development of small foci of immature woven trabecular bone (Fig. 4E,F). At the 10-day time point PF, the healing callus was larger and the fractured bones were more aligned with greater approximation of the fractured ends (Fig. 4G) compared to the healing callus at earlier time points. The healing callus at the 10-day time point also demonstrated increased maturation of the callus with more mature osteoid matrix and trabecular bone-like structures (Fig. 4H,I).

These data were further confirmed using Masson's trichrome staining (Fig. 5). There was an absence of collagen fibers in the healing callus at earlier 5-day time point PF, consistent with an aggregation of differentiating MSCs (Fig. 5A–C). We noticed that collagen fibers, stained blue, had started to appear in the healing callus at 7-day PF and were arranged in multiple irregular nodules, which were stained a faint blue (Fig. 5D–F). These nodules were organized into trabecular-like structures and were stained a dark blue by 10-day PF (Fig. 5G–I). Collectively, these data confirm the development of healing callus at 7-day PF that matures further by 10-day PF into woven trabecular bone and ossification sites.

ANALYSIS OF OA mRNA EXPRESSION IN POST-FRACTURE CALLUS

To explore OA expression during fracture repair, we used an OA cDNA as a probe for Northern blot analysis. We prepared a nylon membrane with total RNA samples isolated at different days PF (days 3, 5, 7, 10, 14, and 21), from three different PF calluses and three different intact femurs (included bone marrow and normal growth plate cartilage). These time points coincide, respectively, with the various cellular events that occur during fracture healing: soft callus formation (cartilage tissue), hard callus formation (osteoid formation under periosteum), endochondral and intramembranous ossifications, and osteoclast remodeling of the new bone [Jingushi et al., 1992].

As shown in Figure 6A, the 1.2 kb OA mRNA transcript was expressed at low levels in the intact femurs (no fracture, lane 1), but highly expressed in PF days 3, 5, and 10 calluses (lanes 2, 3, and 5). OA mRNA expression increased as early as PF day 3, peaking at PF day 10, and declined by PF days 14 and 21 (Fig. 6A). The relative levels of OA mRNA during the development of the fracture callus were determined by IOD measurements normalized to that of 18S

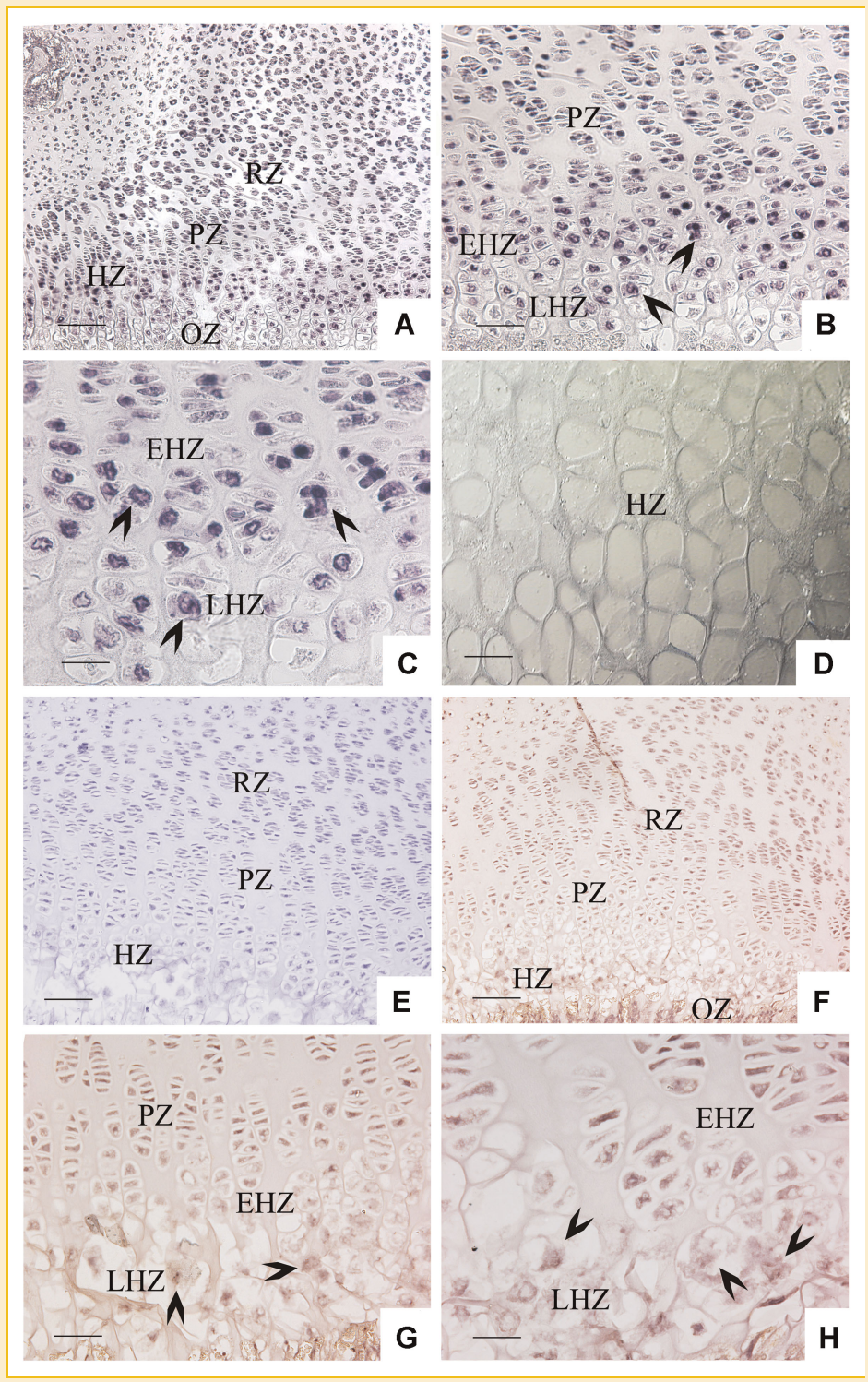

Fig. 3. In situ hybridization and immunolocalization of OA in the growth plate. Sections of the tibial growth plate from 2-week-old male rats were processed for ISH with DIG-labeled OA antisense (A–C), or immunostained with antibodies specific for OA (F–H). Sections incubated with OA sense riboprobe (D) or not incubated with OA antibody (E) were used as negative control. Note that dark blue signal indicative of OA mRNA or brown reaction product indicative of OA protein is localized predominantly in the early hypertrophic zone, zone of late hypertrophic, and terminally differentiated chondrocytes (arrows). Note the absence of blue signal and brown reaction product in the proliferative zone. RZ, resting zone; PZ, proliferative zone; HZ, hypertrophic zone; EHZ, early hypertrophic zone; LHZ, late hypertrophic zone; OZ, ossification zone. Scale bar shown (50 μM). [Color figure can be viewed in the online issue, which is available at wileyonlinelibrary.com.]

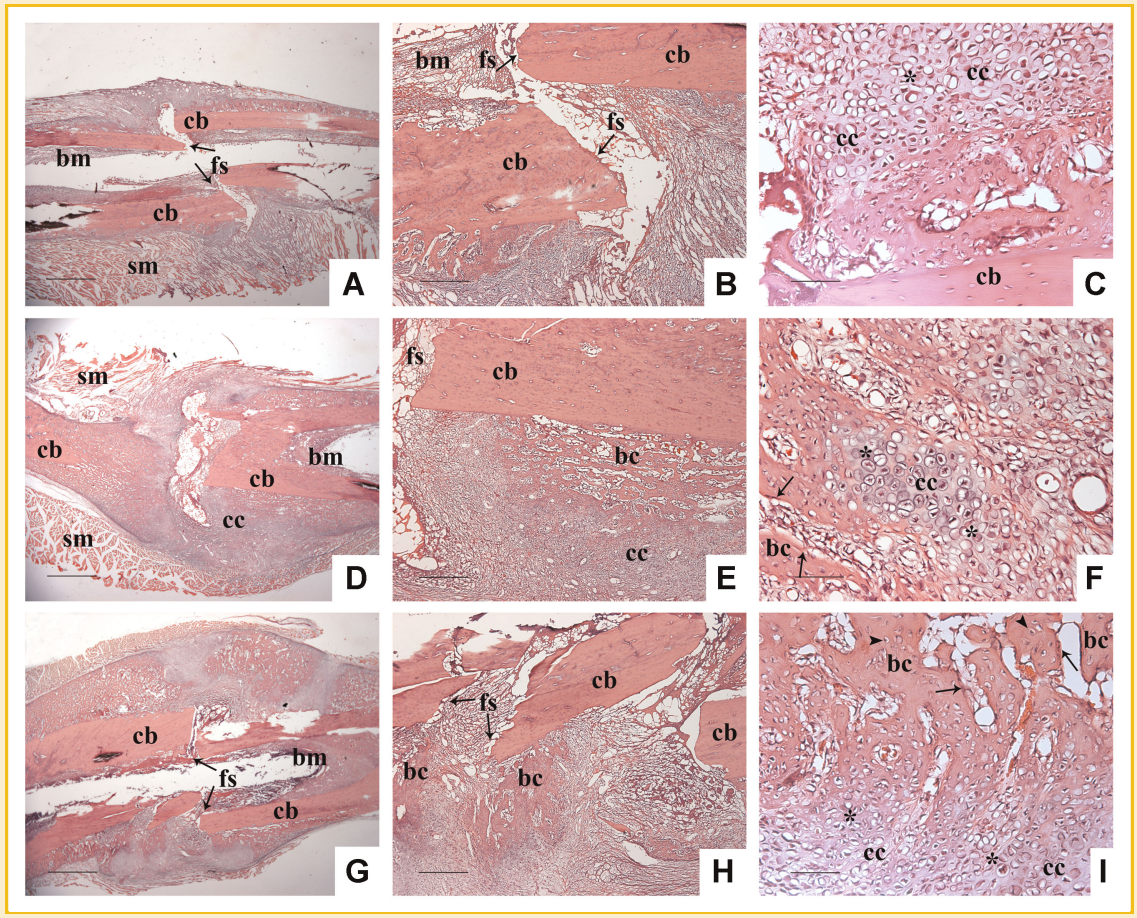

Fig. 4. Hematoxylin and eosin staining of fracture repair. Sections of fractured femoral diaphyses and calluses formed at different time points PF were processed for staining with hematoxylin and eosin. A–C: Photomicrographs of sections were taken from fracture sites at 5 days PF. D–F: Photomicrographs of sections were taken from fracture sites at 7 days PF showing the islets of blue stained hypertrophic chondrocytes indicative of cartilaginous callus. G–I: Photomicrographs of sections were taken from fracture sites at 10 days PF showing the woven bone trabeculae, stained with red, indicative of bony callus. fs, fracture site; cc, cartilaginous callus; bc, bony callus; cb, cortical bone; bm, bone marrow; sm, skeletal muscles. Arrows indicate examples of osteoblasts; arrowheads indicate examples of osteocytes; asterisks indicate examples of hypertrophic chondrocytes. Scale bar shown (50 μM). [Color figure can be viewed in the online issue, which is available at wileyonlinelibrary.com.]

rRNA (Fig. 6B). When compared with intact bone, OA mRNA expression in the callus was increased approximately 2.5-fold by PF day 3, was increased to 3.2-fold by PF day 10, and then declined to 1.5-fold by PF days 14 and 21, which was still higher than in intact bone (Fig. 6B).

To investigate whether OA expression corresponded with active osteogenesis where osteoblasts are active in bone formation, we examined the expression of osteocalcin mRNA at the same PF time points. Similar to OA expression levels, the highest level of osteocalcin was detected at PF day 10 indicating an active bone formation at this time point (data not shown).

To confirm results of Northern blot analysis and to demonstrate OA mRNA expression by hypertrophic chondrocytes, pre- and newly developed osteoblasts, we used DIG-labeled OA antisense riboprobe for in situ hybridization in the PF day 3, 5, 7, 10, 14, and 21 calluses. Paraffin sections of day-3 PF calluses showed the beginning of callus formation at the fracture site, with an aggregation of MSCs (Fig. 7A–C). At day 3, the positive OA signals (blue) were localized to almost all cell types, compared to unfractured control femurs from the contralateral limb (data not shown). At day 5, the PF callus showed that positive OA signals were more localized to islands of immature cells ready to differentiate with the development of cartilaginous callus (Fig. 7D–F). The PF callus at day 7 showed well-localized signals in chondrocytes and some osteoblasts, based on cell morphology, within the maturing cartilaginous callus (Fig. 7G–I). The PF callus at day 10 showed a well-established bony callus with newly developed osteoblasts and osteocytes expressing intense OA signals (Fig. 7J–L), compared to less intense signals expressed by osteoblasts at day-7 PF callus. Interestingly, quantitative analysis of OA signals in multiple sections at different time points PF showed that OA expression was increased 4.2-fold at 3-day PF, and reached the highest expression of 5.1-fold at 10-day PF compared to the unfractured controls (Table I). OA expression level was the lowest at day-21 PF (1.6-fold greater than unfractured controls) (Table I).

ANALYSIS OF OA PROTEIN EXPRESSION IN POST-FRACTURE CALLUS

To support the previous in situ hybridization data and to confirm the cellular location of OA in the fracture callus, we decided to analyze OA protein expression via immunocytochemistry in the

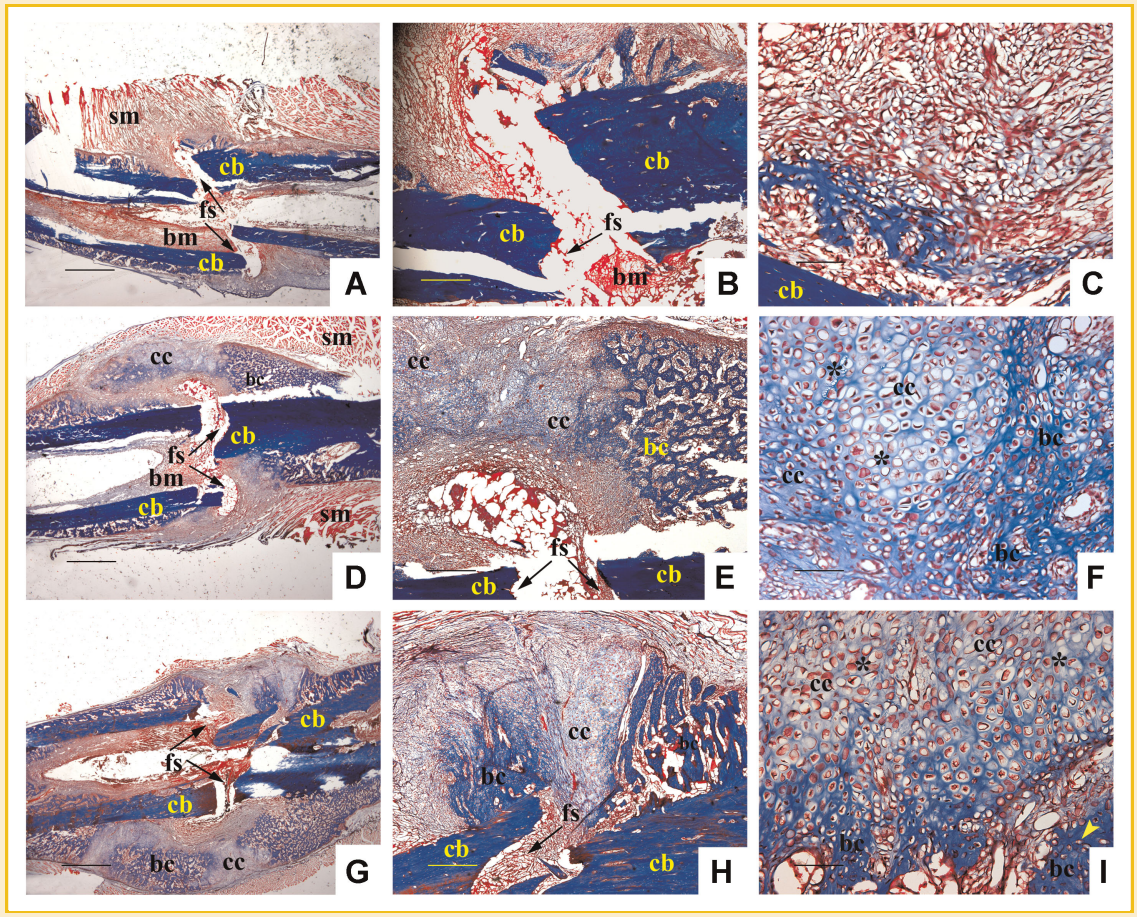

Fig. 5. Masson's trichrome staining of fracture repair. Sections of fractured femoral diaphyses and calluses formed at different time points PF were processed for Masson's trichrome staining. A–C: Photomicrographs of sections were taken from fracture sites at 5 days PF. D–F: Photomicrographs of sections were taken from fracture sites at 7 days PF showing the islets of hypertrophic chondrocytes indicative of cartilaginous callus, stained with faint blue. G–I: Photomicrographs of sections were taken from fracture sites at 10 days PF showing the woven bone trabeculae stained with dark blue. fs, fracture site; cc, cartilaginous callus; bc, bony callus; cb, cortical bone; bm, bone marrow; sm, skeletal muscles. Arrows indicate examples of osteoblasts; arrowheads indicate examples of osteocytes; asterisks indicate examples of hypertrophic chondrocytes. Scale bar shown (50 μM). [Color figure can be viewed in the online issue, which is available at wileyonlinelibrary.com.]

calluses at days 3, 5, 7, 10, 14, and 21 PF. In the numerous immunostained sections used from each time point PF; we observed strong labeling for OA throughout the entire soft and hard callus (i.e., PF days 5 and 10, respectively; Fig. 8). Specifically, the OA protein was strongly detected in the cytoplasm of aggregated immature stromal and MSCs at day-3 PF consistent with subsidence of inflammation and beginning of callus formation (Fig. 8A–C). Moreover, OA immunoreactivity was more localized to osteoprogenitor cells (pre-osteoblasts) in the fibrous periosteum at day-5 PF (Fig. 8D–F). Interestingly, strong OA immunoreactivity was observed in hypertrophic chondrocytes at day-7 PF that coincide with the development of cartilaginous soft callus (Fig. 8G–I). Furthermore, OA immunoreactivity was more localized in osteoblasts that coincide with hard callus formation. Paraffin sections at day-14 and -21 PF showed strong OA immunoreactivity in the cytoplasm of active osteoblasts lining the surfaces of newly developed trabecular bone, and in osteocytes embedded in the newly made woven bone during intramembranous ossification (Fig. 8M–R). We noticed that OA immunoreactivity was present not only in osteoblasts and osteocytes at day-14 and -21 PF but also in the osteoid matrix surrounding these cells, (Fig. 8M–R). On the other hand, we noticed strong OA immunoreactivity in the cytoplasm of large differentiated osteoclasts (>3 nuclei). An adjacent section stained with secondary antibody alone (servly as a negative control) resulted in sections without any labeling (data not shown). Quantitative analysis of the OA immunoreactivity showed that OA expression was 3.3-fold increased at 3-day PF and reached the highest expression of 4.1-fold at 10-day PF compared to unfractured controls (Table I). Level of OA expression was the lowest at day-21 PF (1.3-fold greater than unfractured controls). Collectively, these data confirmed the expression of OA mRNA and protein by osteoblasts, osteocytes, and chondrocytes during the healing process PF, suggesting an important role for OA in endochondral and intramembranous bone formations during fracture repair.

DISCUSSION

Detection of various growth factors, such as BMPs, TGF-β, bFGF, and PDGF, have been previously reported in osteoblasts lining bone

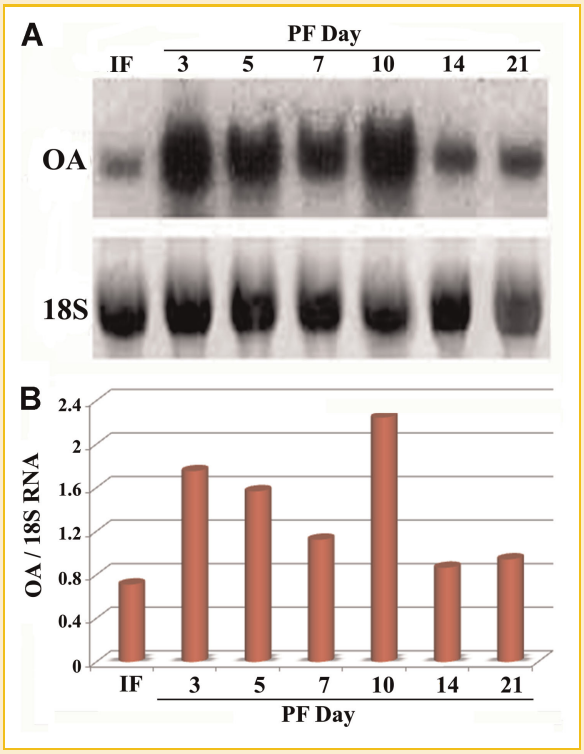

Fig. 6. Temporal expression of OA mRNA during fracture healing. A: Total RNA (20 μg) was isolated from three different calluses (n = 3) at 3, 5, 7, 10, 14, and 21 days PF, and three different intact femurs, was fractionated on a 1% formaldehyde/agarose gel and Northern blot analysis was carried out as described in the Materials and Methods Section using random labeled OA probes. B: Densitometry of the Northern blot indicating the relative ratio (in arbitrary units) of OA mRNA to that of 18S rRNA in intact femurs (IF) versus healing calluses at different days PF, based on IOD measurements of bands shown in panel A. [Color figure can be viewed in the online issue, which is available at wileyonlinelibrary.com.]

trabecular surfaces in vivo that suggest a potential role for these factors in active bone formation and repair [Sandberg et al., 1993; Tatsuyama et al., 2000; Schmid et al., 2009]. Whether other factors are also involved in bone formation and repair is still under investigation. In the present study, we localized the expression of an osteogenic factor, OA, in intact bone and during fracture healing. We demonstrated that OA is highly expressed in hypertrophic chondrocytes localized in the epiphyseal growth plate and soft fracture callus, and in osteoblasts lining bone trabeculae and in the hard fracture callus.

Interestingly, localization of OA mRNA by in situ hybridization showed high-intensity signal in the osteoblasts lining bone trabeculae in the metaphyseal region in intact long bones, suggesting a potential role for OA in bone formation in vivo. In addition, some osteocytes, localized in trabecular bones, demonstrated OA mRNA signal to a lesser extent that may suggest a role for OA in osteocyte function. Previous reports elucidated the vital role of osteocytes in controlling bone remodeling through cell–cell communication with osteoblasts and osteoclasts [Henriksen et al., 2009]. Moreover, some bone marrow cells that could be MSCs showed a faint signal for OA mRNA, suggesting a possible role for OA in osteoblast early cell fate and commitment. Previous reports showed a critical role for other growth and transcription factors, such as BMP-2 and CBFA-1, not only during early osteoblast cell commitment but also during later stages of osteoblast differentiation in vitro [Komori et al., 1997; Komori, 2003; Mishina et al., 2004; Lian et al., 2006]. We have previously reported that MSCs from mice with a natural mutation in OA gene, showed impairment of differentiation into osteoblasts compared to their wild-type MSCs in vitro [Abdelmagid et al., 2008].

Our in situ hybridization data were supported by immunohistochemical and immunofluorescence data confirming the presence of OA protein predominantly in osteoblasts and to a lesser extent in osteocytes. Interestingly, osteoid matrix within the bony trabeculae showed faint signal of OA protein. This later finding correlates with our published data on secretion of OA protein by osteoblasts in vitro [Safadi et al., 2001; Selim et al., 2003; Abdelmagid et al., 2007, 2008].

We have previously reported on the important role of OA in later stages of osteoblast differentiation by neutralizing the secreted OA protein with OA 551-Ab that inhibited osteoblast differentiation markers [Selim et al., 2003; Abdelmagid et al., 2008]. In addition, we showed that OA C-terminal peptide stimulated osteoblast differentiation and mineralization in vitro [Selim et al., 2007]. We have also reported that OA is downstream of BMP-2 signaling to osteoblasts and that OA mediates BMP-2's effects, at least in part, on osteoblast differentiation and function in vitro [Abdelmagid et al., 2007]. In addition, we reported on the marked increase in CBFA-1 expression by one in osteoblasts treated with OA C-terminal peptide in vitro [Selim et al., 2007]. Collectively, from these data, we conclude that OA has an active role in bone formation in vivo, based on OA mRNA and protein expressions by osteoblasts in vivo and supported by the important role of OA in osteoblast differentiation in vitro either directly and/or indirectly through mediating effects of osteogenic factors, such as BMP-2, and/or up-regulating transcription factors, such as CBFA-1.

Surprisingly, localization of OA mRNA expression was not limited to bone cells but was also shown in hypertrophic chondrocytes in the epiphyseal growth plate, cells that are responsible for cartilage calcification prior to endochondral ossification by osteoblasts. Immunohistochemistry data confirmed the localization of OA protein in early and late hypertrophic chondrocytes and in cartilage matrix suggesting a possible role for OA in terminal chondrocyte differentiation. We also observed minimal signal of OA mRNA and protein in the earlier stages of chondrocyte development, putting a question mark on the possible role for OA in early off fate and commitment of chondrocytes.

Fracture callus showed that OA mRNA expression reached the maximal level at day-10 PF and showed similarity to osteocalcin mRNA expression suggesting a potential role for OA in active osteogenesis PF. Knowing that fracture healing is a specialized type of wound healing involving both chondrogenesis (mark of endochondral ossification) and osteogenesis (mark of intramembranous ossification), our data, showing the high expression of OA in soft and hard callus, suggest its key role as an important regulator of these processes. More specifically, expression of OA mRNA and protein was detected as early as 3 days PF and as late as 21 days PF.

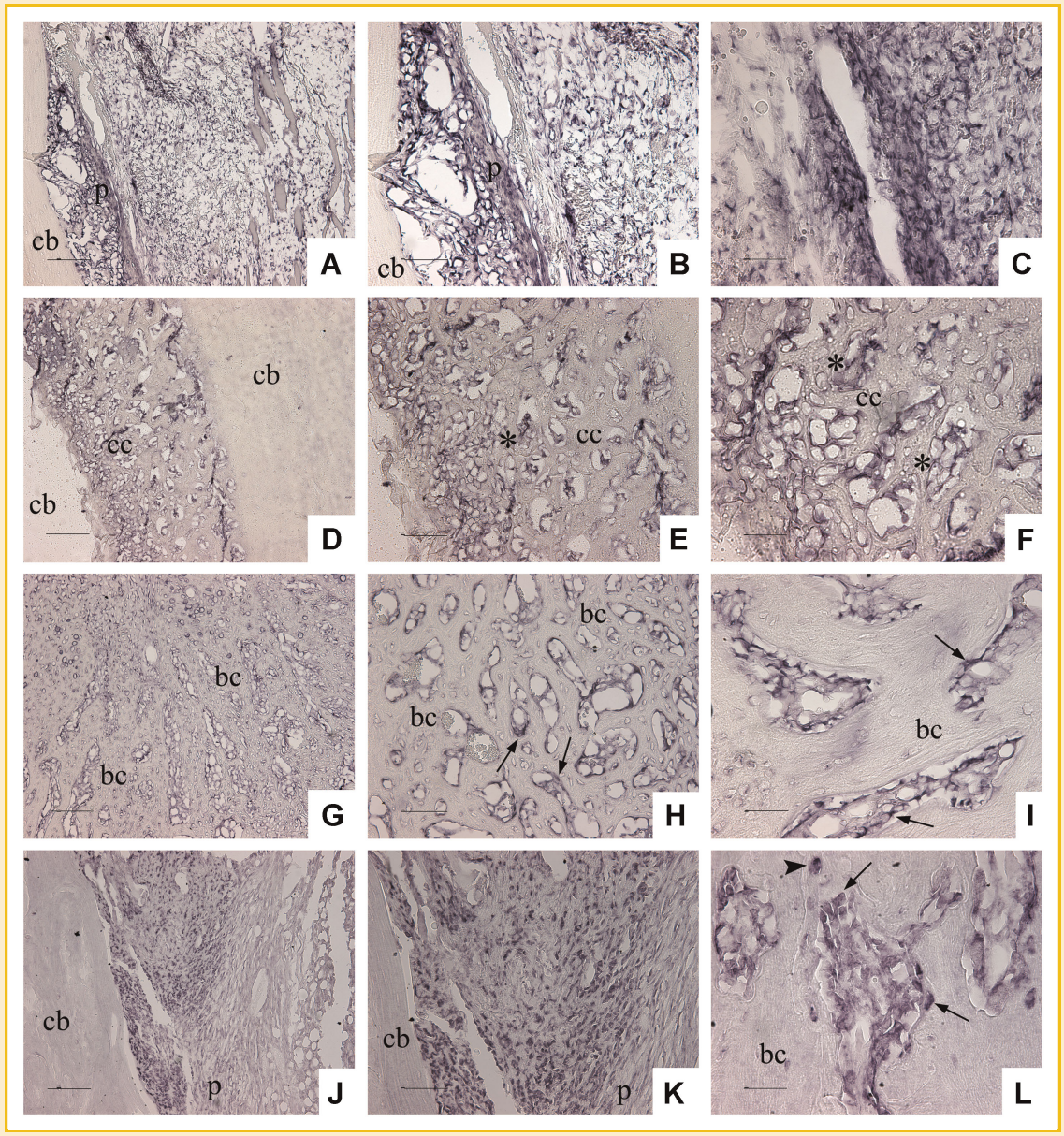

Fig. 7. In situ hybridization of OA during fracture repair. Sections of fractured femoral diaphyses and calluses at different time points PF were processed for ISH using OA antisense riboprobe. A–C: Photomicrographs of sections were taken from fracture sites at 3 days PF showing positive OA mRNA signals (blue) in mesenchymal cells. D–F: Photomicrographs of sections were taken from callus area at 5 days PF showing OA mRNA signals localized into hypertrophic chondrocytes. G–I: Photomicrographs of sections were taken from callus area at 7 days PF. J–L: Photomicrographs of sections were taken from callus area at 10 days PF showing positive OA mRNA signal predominantly associated with newly developed osteoblasts and fainter OA signal localized into osteocytes. fs, fracture site; cc, cartilaginous callus; bc, bony callus; cb, cortical bone; bm, bone marrow. Arrows indicate examples of osteoblasts; arrowheads indicate examples of osteocytes; asterisks indicate examples of hypertrophic chondrocytes. Scale bar shown (50 μM). [Color figure can be viewed in the online issue, which is available at wileyonlinelibrary.com.]

We speculate that OA has a possible role in the early commitment of MSCs in the fracture-healing callus. This is based on the high levels of OA mRNA expression that are detected as early as PF day 3. Furthermore, OA mRNA expression was markedly increased at PF day 5 compared with intact femur that coincide with the most active part of cartilage formation in the callus [Jingushi et al., 1992].

Interestingly, OA mRNA expression was increased within hypertrophic chondrocytes at PF day 5 that coincides with the high expression level of OA mRNA within the hypertrophic zone of the epiphyseal plate growth of intact bones. This finding further suggests a role of the OA gene as a regulator of chondrogenesis. This finding was confirmed at the protein level, whereby OA was detected at high levels in the cytoplasm of hypertrophic chondrocytes of PF day 5 calluses.

On the other hand, OA expression in intact bones was strongly localized in hypertrophic chondrocytes of the epiphyseal growth plate, as well as in osteoblasts, thus accounting for the origin of OA mRNA detected in the intact bone samples (Northern blot analysis).

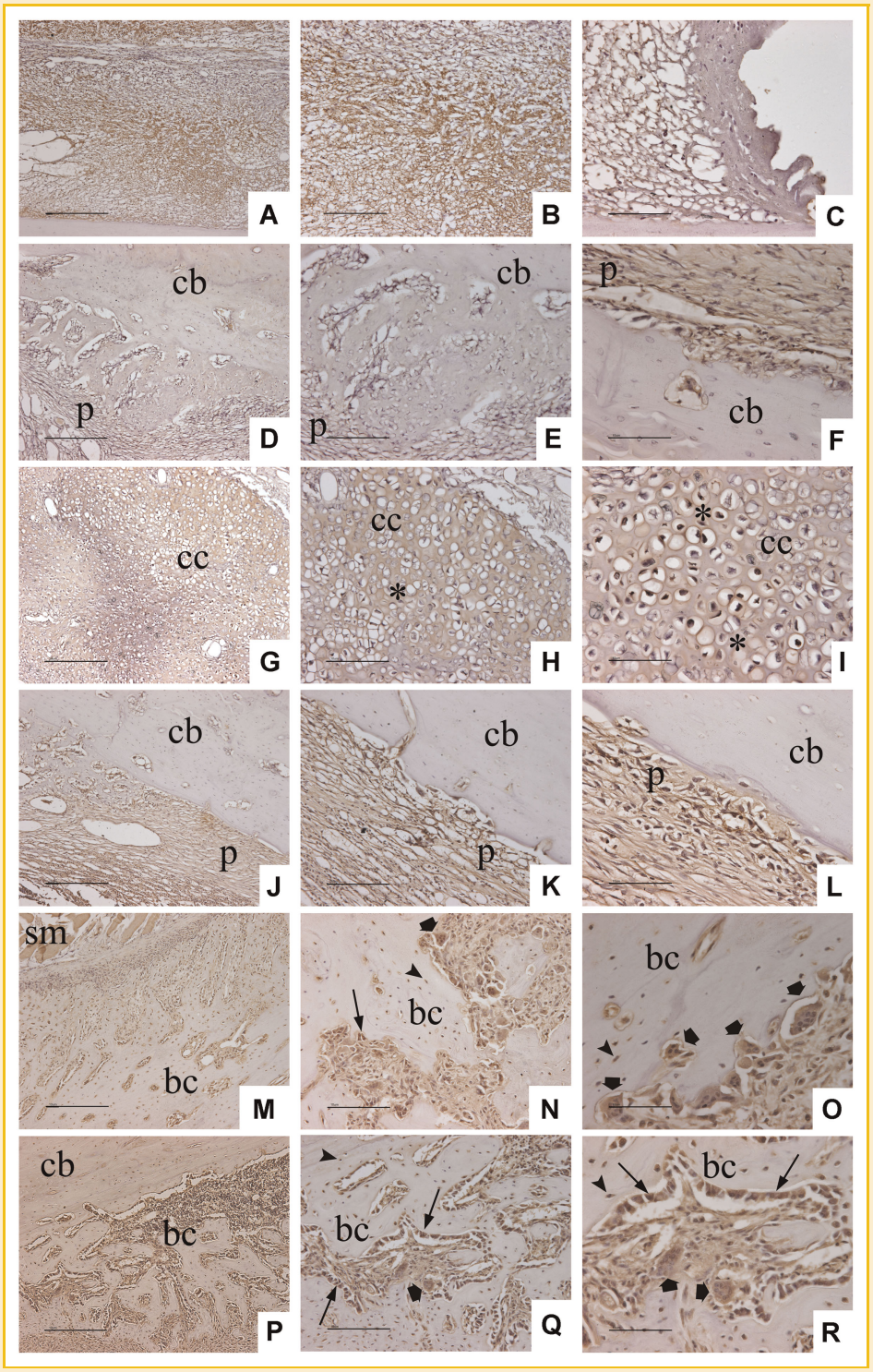

Fig. 8. Immunolocalization of OA during fracture repair. Sections of fractured femoral diaphyses and calluses at different time points PF were immunostained with antibodies specific for OA. A–C: Photomicrographs of sections were taken from fracture sites at 3 days PF showing brown reaction product, indicative of OA protein expression, localized into mesenchymal cells. D–F: Photomicrographs of sections were taken from callus area at 5 days PF showing the OA reaction product localized into osteoprogenitor cells under the periosteum. G–I: Photomicrographs of sections were taken from fracture sites at 7 days PF showing the reaction product localized into hypertrophic chondrocytes. J–L: Photomicrographs of sections were taken from callus area at 10 days PF. M–O: Photomicrographs of sections were taken from callus area at 14 days PF showing the OA reaction product localized into large multinucleated osteoclasts. P–R: Photomicrographs of sections were taken from callus area at 21 days PF showing the OA reaction product is predominantly associated with newly developed osteoblasts and multinucleated osteoclasts in-between. Note fainter OA reaction product in osteocytes. fs, fracture site; cc, cartilaginous callus; bc, bony callus; cb, cortical bone; bm, bone marrow; sm, skeletal muscles. Arrows indicate examples of osteoblasts; arrowheads indicate examples of osteocytes; wide arrows indicate example of osteoclasts; asterisks indicate examples of hypertrophic chondrocytes. Scale bar shown (50 μM). [Color figure can be viewed in the online issue, which is available at wileyonlinelibrary.com.]

Ultimately, it will be essential to determine the function of OA in chondrocytes, whether it has paracrine or autocrine effects on adhesion, proliferation, or differentiation of these cells. OA was also found to be expressed by other cell types, including fibroblasts, osteoblasts, immature osteocytes, and skeletal muscle cells during fracture repair. At the earliest time points examined (PF day 3), intense staining was also detected in the fibrous tissue at, or adjacent to the fracture site, consistent with previous reports showing OA expression by fibroblasts in denervated muscles [Ogawa et al., 2005; Furochi et al., 2007a]. Similarly, OA expression was detected in active osteoblasts within areas of intramembranous and endochondral ossification during fracture repair, as well as in osteoblasts present in metaphyseal trabeculae of intact bone. Moreover, OA mRNA expression was markedly increased at PF day 10 compared with intact femur that coincides with an active osteogenesis in the callus [Sandberg et al., 1989].

OA was also detected not only in newly embedded osteocytes within newly formed woven bone, but also in osteocytes residing in mature cortical bone that may indicate a potential role for OA in osteocyte controlled bone remodeling [Henriksen et al., 2009]. Surprisingly, OA was also detected in osteoclasts during later stages of fracture healing at days 14 and 21, where osteoclasts are needed for bone resorption and remodeling to the original structural integrity [Einhorn, 1998]. Sheng and his group immunodetected OA protein in osteoclasts and have shown that OA expression is up-regulated upon receptor activator of NF kappa B ligand-induced osteoclast differentiation in vitro [Sheng et al., 2008].

We speculate that OA expression is increased exponentially when immature chondrocytes, osteoblasts, osteoclasts, and osteocytes fully differentiate into their corresponding mature cells. Thus, OA might represent a new marker for bone cell differentiation. Labeling of OA protein was also detected in the osteoid matrix of the newly formed woven bone at the fracture callus, indicating the presence of secreted OA protein. This finding is supported by our previous studies that showed expression and secretion of OA by rat primary osteoblasts [Safadi et al., 2001; Selim et al., 2003; Abdelmagid et al., 2007, 2008]. Lastly expression of OA was also detected on the residual skeletal muscle present on each femur, consistent with the previous reports that demonstrated high OA expression in muscles after injury [Ogawa et al., 2005; Furochi et al., 2007b].

We hypothesize that similar to other growth factors (bFGF, PDGF, BMPs, and TGF-β), bone matrix has a rich supply of OA during the development and regeneration of the bony skeleton. The data presented in this article provide strong evidence of the correlation between OA expression in intact bone and fracture repair. Previous data showed that BMP signaling components are expressed in human fracture callus, demonstrated by intense immunoreactivity for BMP-2, -3, -4, and -7, and phosphorylated BMP-receptor-regulated Smads [Kloen et al., 2003]. Moreover, adenoviral transfer of BMP-2 gene enhanced the early stages of healing in a fracture defect rabbit model and increased formation of bone and cartilage [Southwood et al., 2004a,b]. Additionally, micro-CT analysis demonstrated increased bone regeneration in BMP-2 grafted into 5 mm critical sized rat calverial defects [Cowan et al., 2007]. Lastly, mice with deficiency in BMP-2 production in their limb bones demonstrated spontaneous fractures that do not resolve with time. In fact, the earliest steps of fracture healing seem to be blocked in bones deficient in BMP-2, suggesting that BMP-2 has a critical role in the signaling cascade that governs fracture repair [Tsuji et al., 2006]. Looking at OA expression during the fracture healing in these BMP-2 knockout mice will definitely shed light on the role of OA as a downstream mediator of BMP-2 effects during fracture healing.

Previous data indicating that BMPs, TGF-β, bFGF, and PDGF regulate fracture repair [Sandberg et al., 1993; Tatsuyama et al., 2000; Schmid et al., 2009], coupled with the fact that some of these factors (BMP-2, bFGF, and PDGF) regulate OA expression [Ogawa et al., 2005; Abdelmagid et al., 2007] provides evidence for a molecular sequence of events. Thus, after a bone fracture, elevated bFGF could induce OA expression (in osteoblasts and/or chondrocytes) as seen at PF days 3 and 5. As PDGF levels and more specifically BMP-2 levels, dramatically increase during chondrogenesis, these factors probably stimulate a parallel marked increase in OA expression (as seen at PF days 7 and 10), strongly suggesting that these factors can together modulate OA expression at least in part, during cartilage formation.

Taken together, our results demonstrating the intrinsic link between OA expression and biological processes like chondrogenesis and osteogenesis during fracture repair suggest that this gene plays an important role as a key regulator of such events. It is possible then, that OA administered at the proper dose and time during fracture repair, could serve as a potential therapeutic agent in enhancing normal fracture healing as well as impaired fracture repair (e.g., delayed and non-unions).

ACKNOWLEDGMENTS

This research work was supported by grants from the National Institute of Arthritis and Musculoskeletal and Skin Diseases (AR48892), to F.F.S, and Grant from the Department of Health, State of Pennsylvania to F.F.S.

REFERENCES

Abdelmagid SM, Barbe MF, Arango-Hisijara I, Owen TA, Popoff SN, Safadi FF. 2007. Osteoactivin acts as downstream mediator of BMP-2 effects on osteoblast function. J Cell Physiol 210:26–37.

Abdelmagid SM, Barbe MF, Rico MC, Salihoglu S, Arango-Hisijara I, Selim AH, Anderson MG, Owen TA, Popoff SN, Safadi FF. 2008. Osteoactivin, an anabolic factor that regulates osteoblast differentiation and function. Exp Cell Res 314:2334–2351.

Abe H, Uto H, Takami Y, Takahama Y, Hasuike S, Kodama M, Nagata K, Moriuchi A, Numata M, Ido A, Tsubouchi H. 2007. Transgenic expression of osteoactivin in the liver attenuates hepatic fibrosis in rats. Biochem Biophys Res Commun 356:610–615.

Ahn JH, Lee Y, Jeon C, Lee SJ, Lee BH, Choi KD, Bae YS. 2002. Identification of the genes differentially expressed in human dendritic cell subsets by cDNA subtraction and microarray analysis. Blood 100:1742–1754.

Anderson MG, Smith RS, Savinova OV, Hawes NL, Chang B, Zabaleta A, Wilpan R, Heckenlively JR, Davisson M, John SW. 2001. Genetic modification of glaucoma associated phenotypes between AKXD-28/Ty and DBA/2J mice. BMC Genet 2:1.

Anderson MG, Smith RS, Hawes NL, Zabaleta A, Chang B, Wiggs JL, John SW. 2002. Mutations in genes encoding melanosomal proteins cause pigmentary glaucoma in DBA/2J mice. Nat Genet 30:81–85.

Anderson MG, Libby RT, Mao M, Cosma IM, Wilson LA, Smith RS, John SW. 2006. Genetic context determines susceptibility to intraocular pressure elevation in a mouse pigmentary glaucoma. BMC Biol 4:20.

Andrew JG, Hoyland JA, Freemont AJ, Marsh DR. 1995. Platelet-derived growth factor expression in normally healing human fractures. Bone 16: 455–460.

Andriano KP, Chandrashekar B, McEnery K, Dunn RL, Moyer K, Balliu CM, Holland KM, Garrett S, Huffer WE. 2000. Preliminary in vivo studies on the osteogenic potential of bone morphogenetic proteins delivered from an absorbable puttylike polymer matrix. J Biomed Mater Res 53:36–43.

Bandari PS, Qian J, Yehia G, Joshi DD, Maloof PB, Potian J, Oh HS, Gascon P, Harrison JS, Rameshwar P. 2003. Hematopoietic growth factor inducible neurokinin-1 type: A transmembrane protein that is similar to neurokinin 1 interacts with substance P. Regul Pept 111:169–178.

Bonnarens F, Einhorn TA. 1984. Production of a standard closed fracture in laboratory animal bone. J Orthop Res 2:97–101.

Chen WJ, Jingushi S, Aoyama I, Anzai J, Hirata G, Tamura M, Iwamoto Y. 2004. Effects of FGF-2 on metaphyseal fracture repair in rabbit tibiae. J Bone Miner Metab 22:303–309.

Chung JS, Sato K, Dougherty II, Cruz PD, Jr., Ariizumi K. 2007. DC-HIL is a negative regulator of T lymphocyte activation. Blood 109:4320–4327.

Cowan CM, Aghaloo T, Chou YF, Walder B, Zhang X, Soo C, Ting K, Wu B. 2007. MicroCT evaluation of three-dimensional mineralization in response to BMP-2 doses in vitro and in critical sized rat calvarial defects. Tissue Eng 13:501–512.

Einhorn TA. 1998. The cell and molecular biology of fracture healing. Clin Orthop Relat Res 355 suppl:S7–S21.

Furochi H, Tamura S, Mameoka M, Yamada C, Ogawa T, Hirasaka K, Okumura Y, Imagawa T, Oguri S, Ishidoh K, Kishi K, Higashiyama S, Nikawa T. 2007a. Osteoactivin fragments produced by ectodomain shedding induce MMP-3 expression via ERK pathway in mouse NIH-3T3 fibroblasts. FEBS Lett 581: 5743–5750.

Furochi H, Tamura S, Takeshima K, Hirasaka K, Nakao R, Kishi K, Nikawa T. 2007b. Overexpression of osteoactivin protects skeletal muscle from severe degeneration caused by long-term denervation in mice. J Med Invest 54:248–254.

Gerstenfeld LC, Cullinane DM, Barnes GL, Graves DT, Einhorn TA. 2003. Fracture healing as a post-natal developmental process: Molecular, spatial, and temporal aspects of its regulation. J Cell Biochem 88:873–884.

Gittens SA, Uludag H. 2001. Growth factor delivery for bone tissue engineering. J Drug Target 9:407–429.

Haralanova-Ilieva B, Ramadori G, Armbrust T. 2005. Expression of osteoactivin in rat and human liver and isolated rat liver cells. J Hepatol 42:565–572.

Henriksen K, Neutzsky-Wulff AV, Bonewald LF, Karsdal MA. 2009. Local communication on and within bone controls bone remodeling. Bone 44: 1026–1033.

Jingushi S, Joyce ME, Bolander ME. 1992. Genetic expression of extracellular matrix proteins correlates with histologic changes during fracture repair. J Bone Miner Res 7:1045–1055.

Kloen P, Di Paola M, Borens O, Richmond J, Perino G, Helfet DL, Goumans MJ. 2003. BMP signaling components are expressed in human fracture callus. Bone 33:362–371.

Komori T. 2003. Requisite roles of Runx2 and Cbfb in skeletal development. J Bone Miner Metab 21:193–197.

Komori T, Yagi H, Nomura S, Yamaguchi A, Sasaki K, Deguchi K, Shimizu Y, Bronson RT, Gao YH, Inada M, Sato M, Okamoto R, Kitamura Y, Yoshiki S, Kishimoto T. 1997. Targeted disruption of Cbfa1 results in a complete lack of bone formation owing to maturational arrest of osteoblasts. Cell 89:755–764.

Kuan CT, Wakiya K, Dowell JM, Herndon JE II, Reardon DA, Graner MW, Riggins GJ, Wikstrand CJ, Bigner DD. 2006. Glycoprotein nonmetastatic melanoma protein B, a potential molecular therapeutic target in patients with glioblastoma multiforme. Clin Cancer Res 12:1970–1982.

Lennerz V, Fatho M, Gentilini C, Frye RA, Lifke A, Ferel D, Wolfel C, Huber C, Wolfel T. 2005. The response of autologous T cells to a human melanoma is dominated by mutated neoantigens. Proc Natl Acad Sci USA 102:16013–16018.

Lian JB, Stein GS, Javed A, van Wijnen AJ, Stein JL, Montecino M, Hassan MQ, Gaur T, Lengner CJ, Young DW. 2006. Networks and hubs for the transcriptional control of osteoblastogenesis. Rev Endocr Metab Disord 7: 1–16.

Mandracchia VJ, Nelson SC, Barp EA. 2001. Current concepts of bone healing. Clin Podiatr Med Surg 18:55–77.

Mishina Y, Starbuck MW, Gentile MA, Fukuda T, Kasparcova V, Seedor JG, Hanks MC, Amling M, Pinero GJ, Harada S, Behringer RR. 2004. Bone morphogenetic protein type IA receptor signaling regulates postnatal osteoblast function and bone remodeling. J Biol Chem 279:27560–27566.

Mo JS, Anderson MG, Gregory M, Smith RS, Savinova OV, Serreze DV, Ksander BR, Streilein JW, John SW. 2003. By altering ocular immune privilege, bone marrow-derived cells pathogenically contribute to DBA/2J pigmentary glaucoma. J Exp Med 197:1335–1344.

Nakamura A, Ishii A, Ohata C, Komurasaki T. 2007. Early induction of osteoactivin expression in rat renal tubular epithelial cells after unilateral ureteral obstruction. Exp Toxicol Pathol 59:53–59.

Ogawa T, Shimokawa H, Fukada K, Suzuki S, Shibata S, Ohya K, Kuroda T. 2003. Localization and inhibitory effect of basic fibroblast growth factor on chondrogenesis in cultured mouse mandibular condyle. J Bone Miner Metab 21:145–153.

Ogawa T, Nikawa T, Furochi H, Kosyoji M, Hirasaka K, Suzue N, Sairyo K, Nakano S, Yamaoka T, Itakura M, Kishi K, Yasui N. 2005. Osteoactivin upregulates expression of MMP-3 and MMP-9 in fibroblasts infiltrated into denervated skeletal muscle in mice. Am J Physiol Cell Physiol 289:C697–C707.

Okamoto I, Pirker C, Bilban M, Berger W, Losert D, Marosi C, Haas OA, Wolff K, Pehamberger H. 2005. Seven novel and stable translocations associated with oncogenic gene expression in malignant melanoma. Neoplasia 7:303–311.

Olsen BR, Reginato AM, Wang W. 2000. Bone development. Annu Rev Cell Dev Biol 16:191–220.

Onaga M, Ido A, Hasuike S, Uto H, Moriuchi A, Nagata K, Hori T, Hayash K, Tsubouchi H. 2003. Osteoactivin expressed during cirrhosis development in rats fed a choline-deficient, L-amino acid-defined diet, accelerates motility of hepatoma cells. J Hepatol 39:779–785.

Origuchi N, Ishidou Y, Nagamine T, Onishi T, Matsunaga S, Yoshida H, Sakou T. 1998. The spatial and temporal immunolocalization of TGF-beta 1 and bone morphogenetic protein-2/-4 in phallic bone formation in inbred Sprague Dawley male rats. In Vivo 12:473–480.

Owen TA, Smock SL, Prakash S, Pinder L, Brees D, Krull D, Castleberry TA, Clancy YC, Marks SC, Jr., Safadi FF, Popoff SN. 2003. Identification and characterization of the genes encoding human and mouse osteoactivin. Crit Rev Eukaryot Gene Expr 13:205–220.

Pollack VA, Alvarez E, Tse KF, Torgov MY, Xie S, Shenoy SG, MacDougall JR, Arrol S, Zhong H, Gerwien RW, Hahne WF, Senter PD, Jeffers ME, Lichenstein HS, LaRochelle WJ. 2007. Treatment parameters modulating regression of human melanoma xenografts by an antibody-drug conjugate (CR011-vcMMAE) targeting GPNMB. Cancer Chemother Pharmacol 60:423–435.

Reddi AH. 1998a. Initiation of fracture repair by bone morphogenetic proteins. Clin Orthop Relat Res 355 suppl:S66–S72.

Reddi AH. 1998b. Role of morphogenetic proteins in skeletal tissue engineering and regeneration. Nat Biotechnol 16:247–252.

Rich JN, Shi Q, Hjelmeland M, Cummings TJ, Kuan CT, Bigner DD, Counter CM, Wang XF. 2003. Bone-related genes expressed in advanced malignancies

induce invasion and metastasis in a genetically defined human cancer model. J Biol Chem 278:15951–15957.

Safadi FF, Xu J, Smock SL, Rico MC, Owen TA, Popoff SN. 2001. Cloning and characterization of osteoactivin, a novel cDNA expressed in osteoblasts. J Cell Biochem 84:12–26.

Sandberg M, Vuorio T, Hirvonen H, Alitalo K, Vuorio E. 1988. Enhanced expression of TGF-beta and c-fos mRNAs in the growth plates of developing human long bones. Development 102:461–470.

Sandberg M, Aro H, Multimaki P, Aho H, Vuorio E. 1989. In situ localization of collagen production by chondrocytes and osteoblasts in fracture callus. J Bone Joint Surg Am 71:69–77.

Sandberg MM, Aro HT, Vuorio EI. 1993. Gene expression during bone repair. Clin Orthop Relat Res 289:292–312.

Schmid GJ, Kobayashi C, Sandell LJ, Ornitz DM. 2009. Fibroblast growth factor expression during skeletal fracture healing in mice. Dev Dyn 238:766–774.

Selim AA, Abdelmagid SM, Kanaan RA, Smock SL, Owen TA, Popoff SN, Safadi FF. 2003. Anti-osteoactivin antibody inhibits osteoblast differentiation and function in vitro. Crit Rev Eukaryot Gene Expr 13:265–275.

Selim AA, Castaneda JL, Owen TA, Popoff SN, Safadi FF. 2007. The role of osteoactivin-derived peptides in osteoblast differentiation. Med Sci Monit 13:BR259–BR270.

Sheng MH, Wergedal JE, Mohan S, Lau KH. 2008. Osteoactivin is a novel osteoclastic protein and plays a key role in osteoclast differentiation and activity. FEBS Lett 582:1451–1458.

Shikano S, Bonkobara M, Zukas PK, Ariizumi K. 2001. Molecular cloning of a dendritic cell-associated transmembrane protein, DC-HIL, that promotes RGD-dependent adhesion of endothelial cells through recognition of heparan sulfate proteoglycans. J Biol Chem 276:8125–8134.

Southwood LL, Frisbie DD, Kawcak CE, Ghivizzani SC, Evans CH, McIlwraith CW. 2004a. Evaluation of Ad-BMP-2 for enhancing fracture healing in an infected defect fracture rabbit model. J Orthop Res 22: 66–72.

Southwood LL, Frisbie DD, Kawcak CE, McIlwraith CW. 2004b. Delivery of growth factors using gene therapy to enhance bone healing. Vet Surg 33:565–578.

Tatsuyama K, Maezawa Y, Baba H, Imamura Y, Fukuda M. 2000. Expression of various growth factors for cell proliferation and cytodifferentiation during fracture repair of bone. Eur J Histochem 44:269–278.

Thompson Z, Miclau T, Hu D, Helms JA. 2002. A model for intramembranous ossification during fracture healing. J Orthop Res 20:1091–1098.

Tse KF, Jeffers M, Pollack VA, McCabe DA, Shadish ML, Khramtsov NV, Hackett CS, Shenoy SG, Kuang B, Boldog FL, MacDougall JR, Rastelli L, Herrmann J, Gallo M, Gazit-Bornstein G, Senter PD, Meyer DL, Lichenstein HS, LaRochelle WJ. 2006. CR011, a fully human monoclonal antibody-auristatin E conjugate, for the treatment of melanoma. Clin Cancer Res 12:1373–1382.

Tsuji K, Bandyopadhyay A, Harfe BD, Cox K, Kakar S, Gerstenfeld L, Einhorn T, Tabin CJ, Rosen V. 2006. BMP2 activity, although dispensable for bone formation, is required for the initiation of fracture healing. Nat Genet 38: 1424–1429.

Wang EA, Israel DI, Kelly S, Luxenberg DP. 1993. Bone morphogenetic protein-2 causes commitment and differentiation in C3H10T1/2 and 3T3 cells. Growth Factors 9:57–71.

Weterman MA, Ajubi N, van Dinter IM, Degen WG, van Muijen GN, Ruitter DJ, Bloemers HP. 1995. nmb, a novel gene, is expressed in low-metastatic human melanoma cell lines and xenografts. Int J Cancer 60:73–81.

Wong WC, Yu Y, Wallace AL, Gianoutsos MP, D HS, Walsh WR. 2003. Use of a polymeric device to deliver growth factors to a healing fracture. ANZ J Surg 73:1022–1027.

Yamaguchi A. 1995. Regulation of differentiation pathway of skeletal mesenchymal cells in cell lines by transforming growth factor-beta superfamily. Semin Cell Biol 6:165–173.